

Numerical Analysis of Single Jet Impinging a Flat and Non-flat Plate

Flávia V. Barbosa[1](✉), Senhorinha F. C. F. Teixeira[2], and José C. F. Teixeira[1]

[1] MEtRICs I&D Centre, School of Engineering, University of Minho, Guimarães, Portugal
flaviab@dem.uminho.pt

[2] ALGORITMI I&D Centre, School of Engineering, University of Minho, Guimarães, Portugal

Abstract. The complexity of the flow field and heat transfer in jet impingement has led to several studies in order to increase the processes and products performance. Jet impingement is widely implemented, since it ensures high average heat transfer coefficients and the uniformity of the temperature over the target surface. However, the flow generated depends on several parameters related to the jet flow, such as jet velocity and temperature, and the target plate geometry. Complex impinging surfaces are identified in the majority of the applications, such as reflow soldering and cooling of turbines or solar systems. To increase the process efficiency, it is important to fully understand the interactions between the jet and the target surface. Considering the interest of this field, the present study is conducted to investigate the influence of the target surface on heat transfer in a single jet impingement process. To minimize the number of experiments, decreasing time and costs, the implementation of numerical tools is fundamental. In that sense, the impingement of the hot air jet over a flat and non-flat plate was predicted numerically using the ANSYS FLUENT software. The velocity and temperature profile were analyzed and the Nusselt number were compared for both cases. The results show the complexity of the flow generated in the vicinity of the step and the changes of the jet flow structure when it impinges a complex surface.

Keywords: Jet impingement · Heat transfer · Non-flat surface

1 Introduction

Jet impingement, a widely used technique in cooling and heating applications, is a complex heat transfer process that ensures high heat transfer rates over the target surface. However, one of the biggest issues of this forced convection process is the difficulty to obtain uniform temperatures over the impinging surface. If the complexity of the surface is increased, more hot/cold spots can appear, leading to product defects. In order to understand the influence of the target plate geometry on heat transfer performance, several studies have been conducted. Spring et al. [1] concluded that the use of large ribs mainly influence the interaction with crossflow to generate locally higher surface crossflow velocities and turbulence in the wake regions between ribs. In terms of ribs shape, Annerfeldt et al. [2] mentioned that triangle-shaped, wing-shaped, cylindrical and rectangular elements enhance the Nusselt number by a factor from 1 to 1.3 for cooling

© Springer Nature Switzerland AG 2020
O. Gervasi et al. (Eds.): ICCSA 2020, LNCS 12253, pp. 487–495, 2020.
https://doi.org/10.1007/978-3-030-58814-4_34

application. Brakmann et al. [3] analyzed the influence of micro cube shaped pins on the target surface and they found that pins increase the target area by 150% comparatively to a flat plate, resulting in an increase of the convective heat transfer between 135% and 142%. In terms of flow field, they observed that when the airflow passes through a pin, it will be separated inducing a vortex on the downstream side of the pin. This leads to a decrease of the heat transfer and to an increase of the pressure loss in this zone. Furthermore, Ligrani et al. [4] studied the influence of small-scale cylinders in the target plate, observing that the increase of the height of small cylinders leads to an increase of the local mixing, vorticity, turbulent thermal transport and thermal resistance, generating a substantial thermal insulation barrier. Buzzard et al. [5] proved that the average Nusselt number is increased by rectangular roughness of small height, since the increase of the height leads to an increase of the local vorticity and larger mixing. In addition, for laminar flows, plates with small roughness alone present higher Nusselt numbers than plates with a combination of small and large roughness. However, the reverse situation is observed when the flow is turbulent. According to Ren et al. [6], this is due to two reasons: first, in turbulent flows, the combination of large and small pins increases the mixing of the flow, increasing the convective heat transfer at the surface; second, in laminar flows, the extra material provided by large rectangles generates an insulating effect.

The numerical modelling of jet impingement has been implemented in several industrial sectors in order to minimize the number of experiments that force to stop entire production lines and involves huge costs and time waste. Several works have been conducted to select the numerical model which predicts with higher accuracy the jet impingement process. Hofman et al. [7] analyzed 13 turbulence models to determine which one predicts better the jet impingement process and they concluded that nearly all the models predict well the wall jet heat transfer, however almost all of them fail in predicting the local heat transfer near the stagnation region. The SST k-ω model with activated transitional flow option seems to be the model that presents the better predictions. Ortega-Casanova & Granados-Ortiz [8] also agreed that SST k-ω is more accurate in single jet impingement modelling, since it predicts the secondary maximum Nusselt number with accuracy. Ozmen & Ipek [9] demonstrated that Realizable k-ω turbulence model is capable to predict the flow and heat transfer characteristics with success in moderate values of nozzle-to-plate distances. Penumadu & Rao [10] revealed that the heat transfer characteristics are better predicted by SST k-ω model essentially due to its ability to accurately handle regions with high pressure gradients. According to these authors, the SST k-ω model was revealed both as accurate and computing time saving in engineering applications. These advantages make this model a good choice for the numerical modelling of jet impingement process.

In order to understand the influence of the target plate geometry on heat transfer performance, a numerical analysis using the Computational Fluid Dynamics software ANSYS FLUENT was performed. This study analyzes two different surfaces, a flat plate and a plate with a step using the SST k-ω turbulence model. Through these numerical simulations, velocity and temperature profiles over the surface are analyzed. The increased complexity of the flow profile due to the step surface is presented, showing the necessity to explore in detail the flow dynamics in the vicinity of non-flat surfaces. Through the numerical model presented in this work, optimization of the target surface

and jet variables can be conducted in future works, in order to enhance the heat transfer over the impinging plate.

The numerical analysis of the jet flow structure, velocity and temperature is relevant for industrial applications that involve complex surfaces, providing a solution to minimize trial and error techniques still widely used in the industrial sector. Through the numerical model, the detailed study of the jet impingement process can be conducted prior manufacturing, and process optimization can be implemented in order to reduce nonuniform heat transfer over the target plate.

2 Numerical Modelling

2.1 Numerical Domain and Boundary Conditions

The computational domain, presented in Fig. 1, consists of a single jet impinging a flat and non-flat surface. The air flows through a circular nozzle, following a uniform velocity distribution, whose value depends on the Reynolds number required in the study, and at a constant temperature of about 120°C. Since the Mach number is below 0.3, the air jet flow is considered incompressible. After the impingement, the air flow escapes through the side walls. Considering this geometry and the flow parameters, the Reynolds number obtained in this study case is approximately 2,000. According to [11], this flow lies in the transition region. No-slip condition was implemented at both nozzle plate and target plate. A constant temperature of 25°C was specified to the target surface and insulated wall was defined at the nozzle plate. Pressure outlet boundary condition with zero initial gauge pressure was applied to the open sides of the domain.

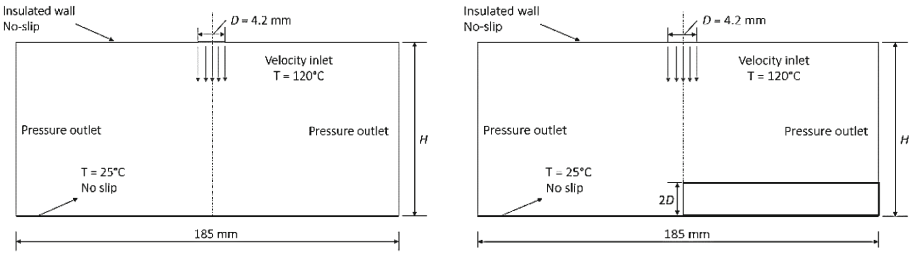

Fig. 1. Numerical domain (a) flat plate (b) step surface.

2.2 Mathematical Model

The governing equations solved by the CFD software FLUENT 19.1 are expressed by Eq. (1) to solve continuity equation, Eq. (2) and Eq. (3) to solve momentum and energy equations, respectively. Since the flow is incompressible, these equations can be written using vectors notation as follows:

$$\nabla \cdot u = 0 \tag{1}$$

$$\frac{\partial u}{\partial t} + u \cdot \nabla u = -\frac{1}{\rho}\nabla p + \mu \cdot \nabla^2 u \tag{2}$$

$$\frac{\partial T}{\partial t} + u \cdot \nabla T = \kappa \cdot \nabla^2 T \tag{3}$$

where u represents the velocity, p the fluid pressure field and T the temperature. The physical properties of the fluid are expressed by the constants ρ, μ and κ which represent the density, kinematic viscosity and diffusivity, respectively.

However, solving full Navier-Stokes equations is too much accurate and demands high computer resources. Since high level of accuracy are not required in this problem, averaged values seem to be enough. The method used to average Navier-Stokes equations is the Reynolds Averaged Navier Stokes (RANS). This method averages the continuity and momentum equations through the decomposition of the velocity by an average velocity (($\bar{u}$) and a fluctuating component $\left(u'\right)$. The unknown velocity fluctuation, u', induces a closure problem which must be solved by using a turbulence model. Considering the advantages pointed out in the previous section, the SST k-ω model was applied to numerically predict the behavior of a jet flow impinging on a flat and non-flat surface. This model, developed by Menter [12], applies the k-ω model in the near wall region and switches to the k-ε model in the far field, combining the advantages of both models. The combination of both SST and the k-ω turbulence models improves the near wall treatment since it gradually switches from a classical low-Reynolds formulation on fine meshes to a log-wall function formulation on coarser grids [13]. The turbulence kinetic energy, k, and the specific dissipation rate, ω, are expressed by Eq. (4) and (5) respectively:

$$\frac{\partial}{\partial t}(\rho k) + \frac{\partial}{\partial x_i}(\rho k u_i) = \frac{\partial}{\partial x_j}\left(\Gamma_k \frac{\partial k}{\partial x_j}\right) + G_k - Y_k + S_k \tag{4}$$

$$\frac{\partial}{\partial t}(\rho \omega) + \frac{\partial}{\partial x_i}(\rho \omega u_i) = \frac{\partial}{\partial x_j}\left(\Gamma_\omega \frac{\partial \omega}{\partial x_j}\right) + G_\omega - Y_\omega + S_\omega \tag{5}$$

where Γ is the effective diffusivity, G and Y are the generation and dissipation of the corresponding variables, respectively, while S_k and S_ω are the user-defined source terms [14].

For the CFD analysis a block-structured grid with 124,500 square elements was used combined with a bias factor of 8, applied near both the target and nozzle plates, which implies a greater refinement close to these walls. This mesh was selected since it ensures a mean wall y^+ value below 2, which according to [15], ensures the accuracy of the SST k-ω model.

The SIMPLE algorithm was used to solve the pressure-velocity coupling. This algorithm uses a relationship between velocity and pressure corrections to enforce mass conservation and to obtain the pressure field [16]. Regarding the spatial discretization of momentum, a second-order upwind was applied while for the dissipation rate and turbulent kinetic energy, a first order upwind was followed. The computational models were solved using a transient formulation based on a first-order implicit method and the convergence criterion of 1E-3 for continuity, momentum and turbulence equations and 1E-6 for energy equation.

3 Results and Discussion

3.1 Velocity Profile

Through the velocity profile, the three main regions identified by Martin [17] can be identified: the free jet region, the stagnation zone and the wall jet region. Between the free jet region and the stagnation zone, another zone can be stated, the decaying region. Viskanta [11] further subdivided this last region in two zones, the initial "developing zone" and the "fully developed zone". The free jet region, formed at the nozzle exit, is characterized by the interaction between the jet and the surrounding environment and presents the maximum velocity value, 12 m/s in this case. As the jet approaches the target plate, it loses axial velocity and turns. A stagnation region is induced, where the overall velocity is near zero [18]. The stagnation region is clearly identified in both flat and non-flat surface. However, as shown in Fig. 2 (b), the step induces a slight deviation of the flow, and an increased mixture between the jet flow and the surrounding air near the bottom of the step was identified. These results are in accordance with [19] and [20], who predicts the separation of the flow at the corner of the step followed by a reattachment downstream on the plate. This phenomenon induces a recirculation region which affects the wall heat transfer. Two stagnation points are identified in this case, located in the bottom and top of the step, while in the flat plate, Fig. 2 (a), this point occur at the jet axis.

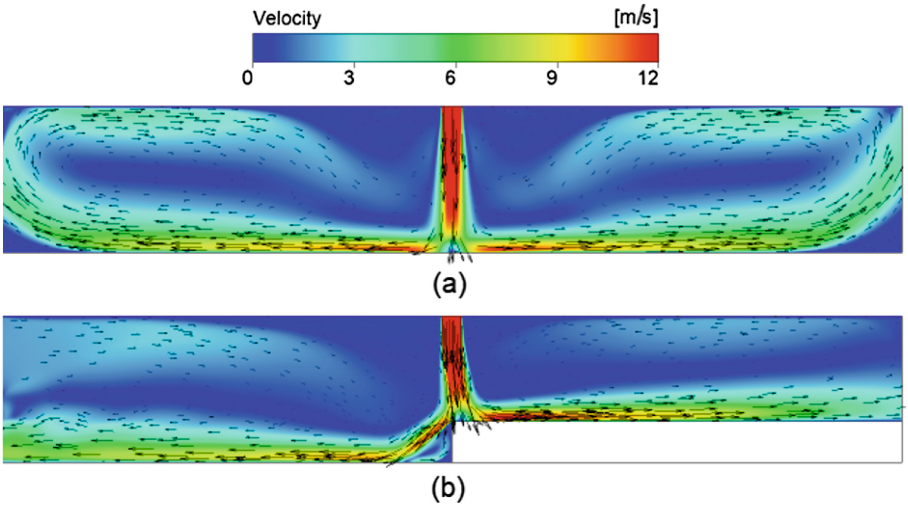

Fig. 2. Jet velocity profile (a) flat plate (b) step surface.

After the contact with the plate, the flow is divided into two streams moving in opposite radial directions along the surface. This wall jet region is characterized by a radial flow with a growing boundary layer [18], due essentially to the strong acceleration of the surrounding flow in the vicinity of the stagnation point. This phenomenon seems to be stronger over the step surface, leading to a flow acceleration and consequently to

a reduction of the boundary layer thickness. Since this boundary layer has a decisive influence for the heat transfer coefficient [21], higher values are expected to be achieved in the non-flat plate case, near the step. The separation of the flow occurs when the boundary layer leaves the surface of the plate. Looking at Fig. 2, it seems that the separation point occurs first in the flat plate, showing that the turbulence generated by the step moves away this point from the centerline of the jet.

3.2 Temperature Profile

The temperature profile, presented in Fig. 3, demonstrated that the uniformization of the temperature field throughout the domain is achieved in the case of a flat plate. However, the step induces higher temperatures in the vicinity of the step, due to the development of a thinner boundary layer compared with the flat plate. In addition, the edge of the step interferes with the boundary layer development, a deceleration of the flow is observed, and consequently a decrease in temperature is identified in this region, which is not observed in the flat plate case. A cold point was also identified in the interface between the flat and step surface. This decrease on temperature can be minimized with a multiple jet impingement configuration. Figure 3 clearly show the shear layer detachment at the step corner, followed by the reattachment, as well as the recirculation vortex induced in the vicinity of the step. As mentioned by [22], this effect induce a decrease of the local heat transfer. These phenomena were also observed experimentally by [20] and [23], and numerically by [19].

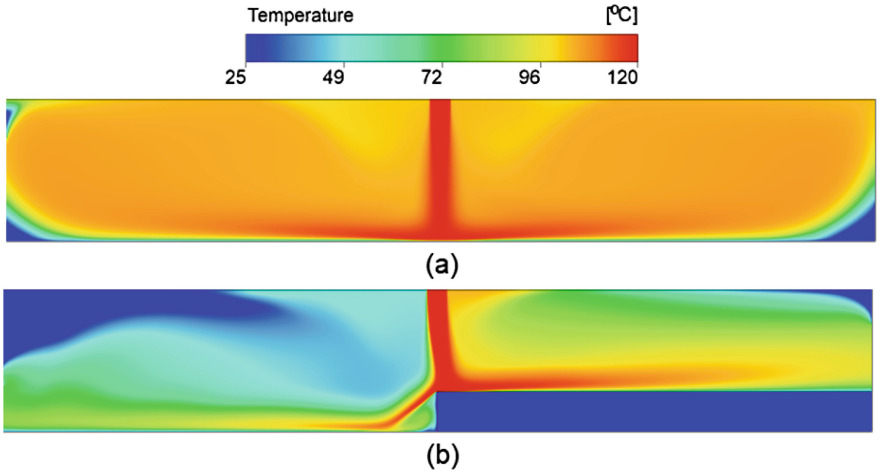

Fig. 3. Temperature profile (a) flat plate (b) step surface.

3.3 Nusselt Number

The Nusselt number variation over the target surface was analyzed and compared for both flat and non-flat plates. Since a larger Nusselt number represents a more effective

convection [24], this property allows to analyze the heat transfer performance of the jet impingement. The Nusselt number, given by Eq. (6), represents the ratio between convection and conduction across a fluid.

$$\mathrm{Nu} = \frac{h \cdot D}{k_{air}} \tag{6}$$

where, D is the jet diameter, k_{air}, the thermal conductivity of the air and h is the local convective heat transfer coefficient, obtained by the ratio between the heat flux by forced convection of the jet flow ($\dot{q}_j$) and the temperature difference between the target surface (T) and the jet at the inlet (T_j), as presented in Eq. (7):

$$h = \frac{\dot{q}_j}{(T - T_j)} \tag{7}$$

The results obtained numerically show the variation of the Nusselt number over the target plate at different jet axis distances. Figure 4 demonstrated that the peak value is reached at the stagnation point located at the jet axis. The step surface induces an increase of the local heat transfer value of approximately 50% compared with a non-flat plate. In terms of heat transfer average, an increase of 10% is observed at $0 < x/D < 2$. This increase due to non-flat surface was also identified in several studies [3, 5, 6, 8]. As mentioned by [23], this is increase is due to small recirculation zones present on the top of the step surface, as well as flow mixing resulting from the separation of flow streamlines near the edge of the upper surface on the step. However, due to the interference of the step edge, lower heat transfer values are recorded near the bottom of the step, essentially due to the recirculation zone. Increasing the distance from this region, the flow develops, and a secondary maximum is recorded at approximately $x/D = -3$. This secondary peak seems to occur due to the transition of the boundary layer from laminar to turbulent. The vortex generated near the bottom edge of the step interferes with the flow, moving away the secondary maximum from the jet axis. These results are in accordance with [20] and

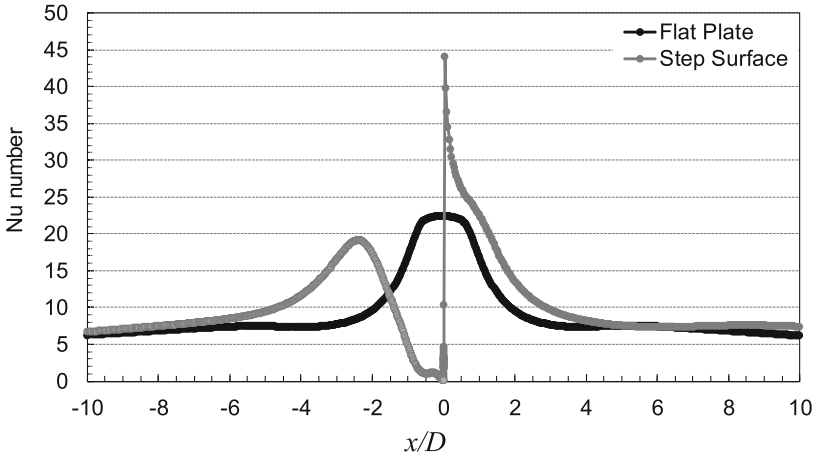

Fig. 4. Nusselt number variation over the target plate.

[23]. The transition region is followed by the wall jet region were a similar decrease of the Nusselt number is observed [25].

4 Conclusions

This work presents a numerical analysis of a single jet impinging a flat and non-flat surface. The results demonstrated the accuracy of the SST k-ω model, since the different regions of the jet were predicted with accuracy. The stagnation point, which is generally the most critical point to be numerically predicted, was clearly identified in both cases. The results show that the step surface generated an acceleration of the flow in the vicinity of the wall, leading to an increase of the heat transfer average of approximately 10% at a jet axis distance (x/D) between 0 and 2. The velocity and temperature profiles show that the step surface induce an acceleration of the flow in the vicinity of the step compared with the flat plate, leading to higher heat transfer values. However, in the left side of the step, a higher degradation of the heat transfer is observed compared with the flat plate. This effect can be minimized with a multiple jet configuration, showing that this process is more propitious to achieve uniform heat transfer profiles over the target surface, minimizing cold and hot spots.

Acknowledgments. The first author would like to express her gratitude for the support given by the Portuguese Foundation for Science and Technology (FCT) and the MIT Portugal Program. This work has been supported by FCT – Fundação para a Ciência e Tecnologia within the R&D Units Project Scope: UIDB/00319/2020 (ALGORITMI Center) and R&D Units Project Scope UIDP/04077/2020 (METRICS Center).

References

1. Spring, S., Xing, Y., Weigand, B.: An experimental and numerical study of heat transfer from arrays of impinging jets with surface ribs. J. Heat Transf. **134**(8), 082201 (2012)
2. Annerfeldt, M.O., Persson, J L., Torisson, T.: Experimental investigation of impingement cooling with tubulators or surface enlarging elements. In: Proceeding of ASME Turbo Expo 2001, New Orleans, Louisiana, USA, 2001-GT-0149, pp. 1–9 (2001)
3. Brakmann, R., Chen, L., Weigand, B., Crawford, M.: Experimental and numerical heat transfer investigation of an impinging jet array on a target plate roughened by cubic micro pin fins. J. Turbomach. **138**(11), 111010 (2016)
4. Ligrani, P.M., Ren, Z., Buzzard, W.C.: Impingement jet array heat transfer with small-scale cylinder target surface roughness arrays. Int. J. Heat Mass Transf. **107**, 895–905 (2017)
5. Buzzard, W.C., Ren, Z., Ligrani, P.M., Nakamata, C., Ueguchi, S.: Influences of target surface small-scale rectangle roughness on impingement jet array heat transfer. Int. J. Heat Mass Transf. **110**, 805–816 (2017)
6. Ren, Z., Buzzard, W.C., Ligrani, P.M., Nakamata, C., Ueguchi, S.: Impingement jet array heat transfer: target surface roughness shape, reynolds number effects. J. Thermophys. Heat Transf. **31**(2), 346–357 (2017)
7. Hofmann, H.M., Kaiser, R., Kind, M., Martin, H.: Calculations of steady and pulsating impinging jets - an assessment of 13 widely used turbulence models. Numer. Heat Transf. Part B Fundam. **51**(6), 565–583 (2007)

8. Ortega-Casanova, J., Granados-Ortiz, F.J.: Numerical simulation of the heat transfer from a heated plate with surface variations to an impinging jet. Int. J. Heat Mass Transf. **76**, 128–143 (2014)
9. Ozmen, Y., Ipek, G.: Investigation of flow structure and heat transfer characteristics in an array of impinging slot jets. Heat Mass Transf. **52**(4), 773–787 (2015). https://doi.org/10.1007/s00231-015-1598-z
10. Penumadu, P.S., Rao, A.G.: Numerical investigations of heat transfer and pressure drop characteristics in multiple jet impingement system. Appl. Therm. Eng. **110**, 1511–1524 (2017)
11. Viskanta, R.: Nusselt-reynolds prize paper - heat transfer to impinging isothermal gas and flame jets. Exp. Therm. Fluid Sci. **6**, 111–134 (1993)
12. Menter, F.R.: Two-equation eddy-viscosity turbulence models for engineering applications. AIAA J. **32**(8), 1598–1605 (1994)
13. Menter, F.R., Ferreira, J.C., Esch, T.: The SST turbulence model with improved wall treatment for heat transfer predictions in gas turbines. Int. Gas Turbine Congr. **2003**(1992), 1–7 (2003)
14. Wen, Z., He, Y., Cao, X., Yan, C.: Numerical study of impinging jets heat transfer with different nozzle geometries and arrangements for a ground fast cooling simulation device. Int. J. Heat Mass Transf. **95**, 321–335 (2016)
15. Xing, Y., Spring, S., Weigand, B.: Experimental and numerical investigation of heat transfer characteristics of inline and staggered arrays of impinging jets. J. Heat Transf. **132**(9), 092201 (2010)
16. Ferziger, J.H., Peric, M.: Computational Methods for Fluid Dynamics, 3rd edn. Springer, USA (1996). https://doi.org/10.1007/978-3-642-97651-3
17. Martin, H.: Heat and mass transfer between impinging gas jets and solid surfaces. Adv. Heat Transf. **13**, 1–60 (1977)
18. Ben Kalifa, R., Habli, S., Saïd, N.M., Bournot, H., Le Palec, G.: Parametric analysis of a round jet impingement on a heated plate. Int. J. Heat Fluid Flow **57**, 11–23 (2016)
19. Behnia, M., Ooi, A., Gregory, P.: Prediction of turbulent heat transfer in impinging jet geometries. Modell. Simul. Turbulent Heat Transf. **15**, 147–175 (2006)
20. Lee, D.H., Chung, Y.S., Ligrani, P.M.: Jet impingement cooling of chips equipped with multiple cylindrical pedestal fins. J. Electron. Packag. Trans. ASME **129**(3), 221–228 (2007)
21. Zuckerman, N., Lior, N.: Jet impingement heat transfer: physics, correlations, and numerical modeling. Adv. Heat Transf. **39**(06), 565–631 (2006)
22. Xu, P., Sasmito, A.P., Qiu, S., Mujumdar, A.S., Xu, L., Geng, L.: Heat transfer and entropy generation in air jet impingement on a model rough surface. Int. Commun. Heat Mass Transf. **72**, 48–56 (2016)
23. Chung, Y.S., Lee, D.H., Ligrani, P.M.: Jet impingement cooling of chips equipped with cylindrical pedestal profile fins. J. Electron. Packag. Trans. ASME **127**(2), 106–111 (2005)
24. Cengel, Y.A., Ghajar, A.J.: Heat and Mass Transfer: Fundamentals and Applications, Fifth Edit. McGraw-Hill Education, New York (2011)
25. Barbosa, F.V., Teixeira, S F C F., Teixeira J.C.F.: Influence of the nozzle-to-plate distance in a jet impinging a cold plate – a numerical approach. In.: Proceeding of ECOS 2019 - The 32nd International Conference on Efficiency, Cost, Optimization, Simulation and Environmental Impact of Energy Systems (2019)